Thermal Protection System preliminary design of STRATOFLY high-speed propelled vehicle

ICAS 2020 SHANGHAI
International Council of the Aeronautical Sciences
32nd Congress of the International Council of the Aeronautical Sciences
September 6-10, 2021
Pudong Shangri-La, Shanghai, China

THERMAL PROTECTION SYSTEM PRELIMINARY DESIGN OF STRATOFLY HIGH-SPEED PROPELLED VEHICLE

Roberto Scigliano[1*], Valeria De Simone[1] , Marco Marini[1],
Roberta Fusaro[2], Davide Ferretto[2], Nicole Viola[2]

[1] Italian Aerospace Research Centre (CIRA), Capua Italy

[2]Politecnico di Torino (PoliTO), Turin, Italy

Abstract

This paper discloses the methodology and the preliminary results achieved in the framework of the H2020 STRATOFLY Project on the design of the Thermal Protection System of the MR3 vehicle. The results of the aero-thermal assessment performed throughout the trajectory clearly indicate the air-intake leading edges as the most critical area, thus dedicated Thermal Protection System alternatives have been explored. Specifically, solutions coupling high-temperature materials (mainly CMC and tungsten with different emissivity paints) with Liquid Metals Heat Pipe arrangements are modelled. Eventually, the effectiveness of the designed solutions is verified with detailed numerical simulation. The design which includes the air-intake main structure made of CMC material and integrating Nickel - Potassium heat pipe results to be the most promising solution to withstand the high thermal loads experienced by STRATOFLY MR3 throughout its Mach 8 long-haul route.

Keywords: hypersonic civil transport, thermal protection system, liquid metal heat pipe

1. Introduction

The worldwide incentive to reconsider commercial hypersonic transport urges Europe to assess the potential of civil high-speed aviation with respect to technical, environmental, and economic viability in combination with human factors, social acceptance, implementation, and operational aspects. In this context, one of the main technical challenges is certainly represented by the high thermal loads experienced by the aircraft throughout the mission. Investigations carried out in a series of EC-funded research projects have permitted maturing a number of feasible hypersonic aircraft configurations, reaching high-level of aero-thermal-propulsive integration: LAPCAT I/II [1], ATLLAS I/II [2], HIKARI, HEXAFLY [3], HEXAFLY-International [4] [5] [6] [7]. In 2018, the European Commission confirmed the financial support to continue these investigations in the context of the H2020 STRATOFLY Project STRATOFLY (Stratospheric Flying Opportunities for High-Speed Propulsion Concepts). Benefitting from the heritage of the previous European projects and selecting the LAPCAT MR2.4 (Mach 8 waverider vehicle) vehicle and mission concept as reference, the H2020 STRATOFLY project aims at further investigating the reference concept, through dedicated multi-disciplinary design methodologies, highly integrated subsystems design, high-fidelity simulations, and test campaigns [8]. In addition, socio-economic and environmentally sustainable aspects are specifically investigated [9].

Looking at the configuration, the STRATOFLY MR3 design is driven by its peculiar mission concept, which can be summarized as follows: STRATOFLY MR3 will be able to fly along long-haul routes reaching Mach 8 during the cruise phase at a stratospheric altitude (h > 30,000 m) carrying 300 passengers as payload. Figure 1 shows the STRATOFLY MR3 external configuration and an idealized reference mission profile. STRATOFLY MR3 has a waverider configuration with the engines and related air ducts completely embedded into the airframe and located at the top of the vehicle (dorsal mounted configuration). The integration of the propulsive system at the top of the vehicle allows maximization of the available planform for lift generation without additional drag penalties, thus increasing the aerodynamic efficiency, and it allows optimizing the internal volume. This layout

guarantees furthermore to expand the jet to a large exit nozzle area without the need to perturb the external shape which would lead to extra pressure drag. However, this specific airframe-propulsive integration naturally exposes the air-intake leading edges to extreme local temperatures, during different phases of the mission.

Therefore, this work aims at describing methodology and the preliminary results achieved for the Thermal Protection System (TPS) design of the STRATOFLY MR3 vehicle. In particular, after a short introduction to the reference MR3 Operational Scenario (Section 2), this paper discloses the methodology followed and the main outcomes of the preliminary aerothermal assessment carried out throughout the trajectory (Section 3). This aerothermal assessment clearly indicates the air-intake leading edges as the most critical area, thus dedicated Thermal Protection System alternatives shall be explored. Consequently, specific attention has been devoted to the selection of plausible high-temperature materials to be adopted for the most critical areas (Section 4), even if architectures including active cooling are also considered. Different alternative solutions coupling high-temperature materials (mainly CMC and tungsten with different emissivity paints) with Liquid Metals Heat Pipe arrangements are modelled. Eventually, the effectiveness of the designed solutions is verified with detailed numerical simulation. The design which includes the air-intake main structure made of CMC material and integrating Nickel - Potassium heat pipe results to be the most promising solution to withstand the high thermal loads experienced by STRATOFLY MR3 throughout its Mach 8 long-haul route.

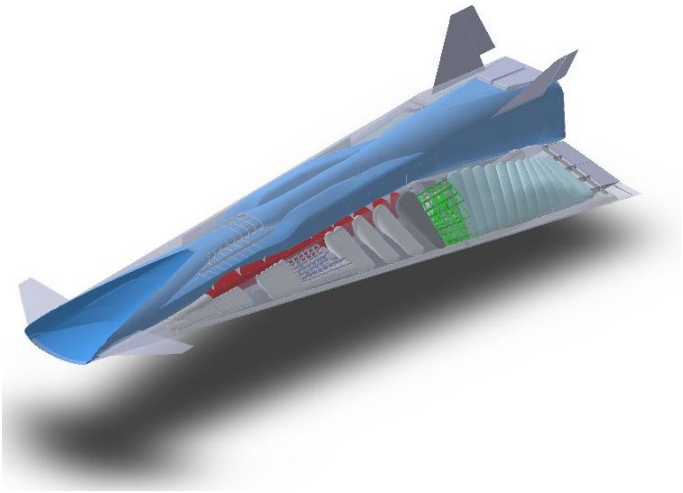

Figure 1 – STRATOFLY MR3 vehicle layout

2. STRATOFLY MR3 Operational Scenario

The very first step to be completed to design a Thermal Protection System is the identification and the analysis of the nominal operational scenario. As anticipated in the introduction, the H2020 STRATOFLY Project has been built on the heritage of the previous European projects and specifically the LAPCAT MR2.4, the most promising Mach 8 waverider concept has been selected as starting point together with its nominal trajectory [10]. Therefore, STRATOFLY MR3 initial set of requirements include the capability to cover a BRU-SYD trajectory in less than 3 hours. Detailed aerodynamic investigations have been performed, aiming at increasing the accuracy of the aero-propulsive databases and a new set of mission simulations [9] have been carried out to verify the possibility to fulfil the initial set of requirements. As reported in [9], thanks to in-depth investigations, the complexity of the aerodynamic model has been increased incrementally, from the sole clean external configuration up to the complete configuration, including propulsion systems elements and flight control surfaces. At each step, the aerodynamic analysis has been complemented with detailed mission analysis, in which the different versions of the aero-dynamic databases have been used as input for the trajectory simulation. However, the structure of the mission remains unchanged: from the horizontal take-off up to Mach 4-4.5, the MR3 is powered by the six Air-Turbo-Rocket (ATR) engines; then the transition to Dual-Mode-Ramjet (DMR) engine allows for a further acceleration to

finally reach cruise conditions (Mach 8 and altitude 32÷33.8 km). The DMR shutdown is foreseen at the end of the cruise, where a gliding deceleration occurs up to the landing. In [6], the possibility to perform a powered descend and landing is mentioned but further investigations are needed. In summary, the expected range to be covered is about 18734 km for a total flight time of less than 3 hours.

Even if, different mission analyses have been run to verify the impact of the more accurate aero-propulsive characterization, in any of the runs, during the entire flight trajectory, the load factors are never critical and the maximum dynamic pressure is always lower than 50 kPa, values reached at the beginning of the cruise. For the sake of simplicity and considering the very limited differences between the different trajectories, in this paper, the original MR2.4 reference trajectory, is kept as reference.

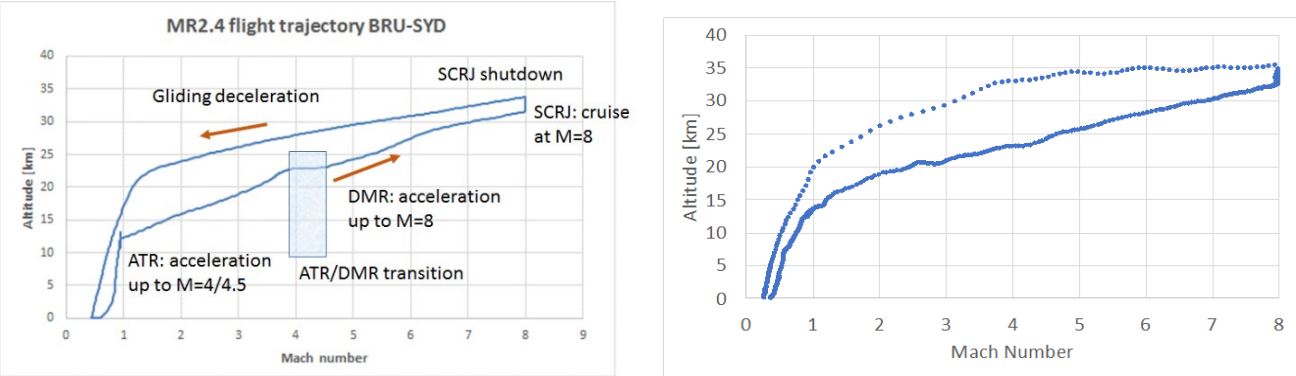

Figure 2 – (a) Reference MR2.4 flight trajectory and (b) MR3 flight trajectory with new aero-propulsive database

3. Aero-thermal assessment throughout the trajectory

Once the reference mission is selected, it is possible to verify the vehicle thermal behavior throughout the trajectory. At this purpose, both engineering formulations, such as the Zoby's model [12] and numerical simulations by means of the Finite Element Methods (FEM).

Specifically, for the purpose of this analysis, a transient thermal analysis throughout the reference trajectory has been performed to evaluate the time dependent temperature of the structure. The procedure adopted for the analysis of the STRATOFLY MR3 vehicle is schematically reported in Fig. 3.

The available CAD model of the vehicle is used to create the numerical model implemented in Ansys Workbench, where the computational mesh is generated. Complementary, a set of stationary CFD calculations have been completed in specific flight conditions to evaluate the convective heat transfer coefficient spatial distribution over the vehicle surface $h(x)|_{CFD_i}$. Eventually, the reference flight trajectory has been split in a certain number of legs, corresponding to one of the specific flight conditions previously analysed through stationary CFD. This allows to keep the effect of both angle of attack and Mach number into account. Indeed, each time leg approximates properly the aerothermal conditions at a specific time instant, in which the exact CFD stationary solution is available, for a certain trajectory time-step. Since CFD solution computes numerically the aerodynamic and aerothermodynamic coefficients which strictly depends by flight parameters such as Mach number, Reynolds, angle of attack etc., this approach implicitly considers flight conditions in the heat transfer coefficient estimation

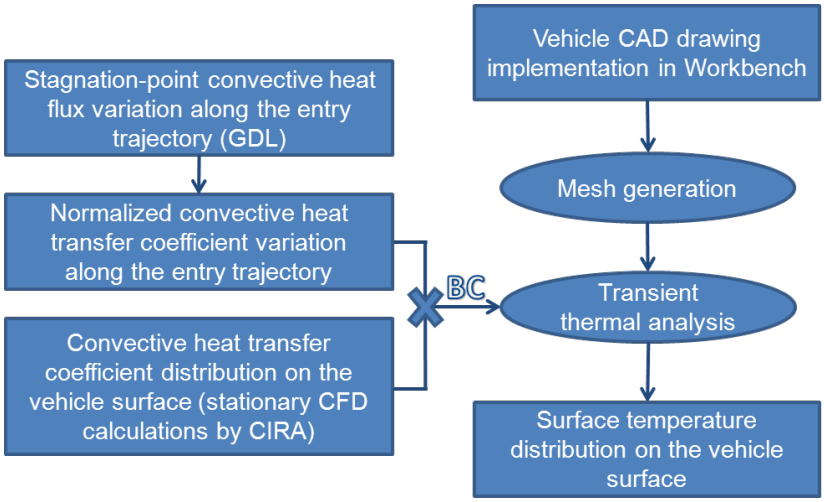

Figure 3 – Transient Thermal Analysis procedure set up for STRATOFLY MR

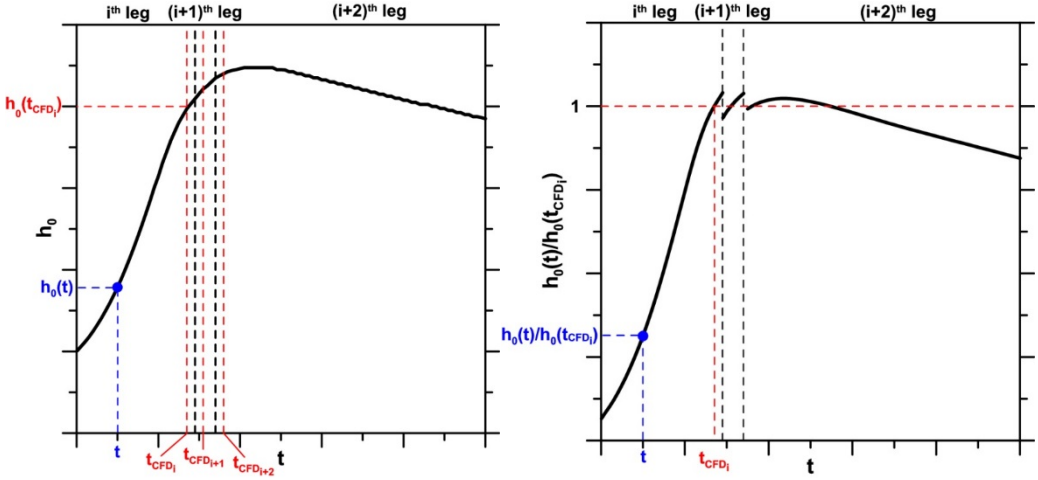

Figure 4: a) Description of CFD results scaling along the trajectory. b) Typical normalized stagnation-point heat transfer function.

For each trajectory leg, the heat transfer coefficient distributions are properly scaled by the stagnation-point heat transfer coefficient variation along the selected trajectory leg, normalized with respect to the corresponding reference condition (i.e. the flight condition analysed by CFD). Referring to the nomenclature reported in Figure 4 a, Eq. (1) is applied.

$$h(x,t) = h(x)|_{CFD_i} \cdot \frac{h_0(t)}{h_0(t_{CFD_i})} \qquad \textbf{(1)}$$

In particular, the stagnation-point convective heat transfer coefficient h(x,t) is estimated by scaling the hot wall stagnation-point convective heat flux variation along the trajectory by the difference between the stagnation temperature (T_0) and the wall temperature profile (T_{wall}), as reported in Eq. (2).

$$h_0 = \frac{\dot{q}_{0,hw}}{T_0 - T_w} \qquad \textbf{(2)}$$

Please, notice that the hot wall stagnation-point convective heat flux variation along the trajectory can also be evaluated according to the Zoby's engineering model. Figure 5 shows the total temperature and the heat transfer coefficient at stagnation points from Zoby calculation and as rebuild on the FEM.

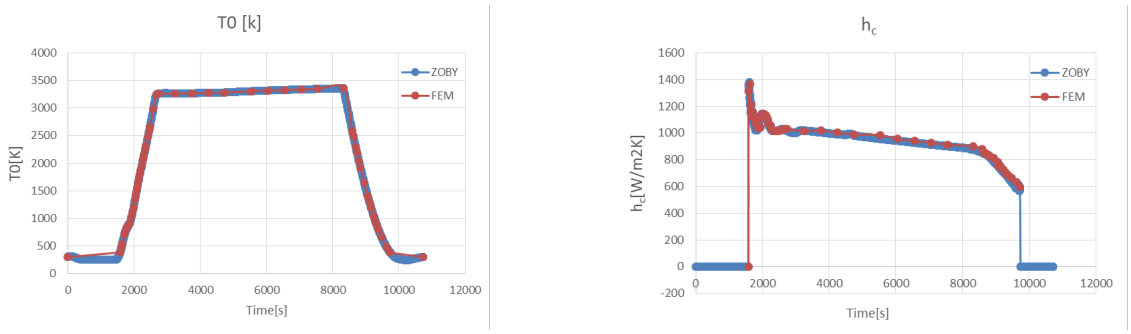

Figure 5: Stagnation temperature profile and heat transfer coefficient profile according to Zoby and rebuilt on the FEM

The transient thermal analysis is then set assuming, as convective boundary condition, the heat transfer coefficient evaluated according to the previously discussed procedure and the stagnation temperature profile (in coherence with the CFD modelling). Please, notice that in addition to the convective heat fluxes, radiative dissipation condition has also been considered for all the external surfaces. Therefore, the overall thermal balance can be written as follows:

$$\dot{q} = h \cdot (T_0 - T_w) - \sigma \cdot \varepsilon \cdot T_w^4 \qquad \textbf{(3)}$$

4. STRATOFLY MR3 Air-intake thermal design

4.1 Air-Intake Heat Pipe preliminary design

As reported in [13][14][15], CMC materials can be widely used for the main structure of STRATOFLY MR3 vehicle and its employment could be considered also for intakes, wing and vertical tail leading edges if the local heat flux does not exceed 0.7 MW/m2. However, for the crotch and the lower lip areas of the air-intakes, an alternative solution, able to withstand the higher expected thermal loads, can be represented by tungsten coated by UHTC (Ultra High Temperature Ceramics Coating). However, this solution may be excessively heavy and thus recommended only for very small applications. Therefore, the authors started investigating the possibility to couple high-temperature material with active cooling strategies. For this specific application, considering the volumetric constraint imposed by the MR3 air-intake, the heat-pipe concept has been further investigated. The typical sizing procedure described in literature [16][17][18] has been used to derive proper heat pipes architecture candidates. Specifically, the adopted process consists in four main steps, described in Figure 6.

Before developing alternative configurations, it has been fundamental to assess the internal thermal environment (see Fig. 7): indeed, the feasible configuration shall combine a reasonable skin thickness with an effective active cooling.

After a set of evaluations, the proposed heat pipe arrangement, which results to be capable of withstanding and managing the heat flux generated by the identified thermal environment is reported in Figure 8, where Potassium (K) has been considered as driving fluid and Nickel (Ni) is selected as material for both primary structure (container) and wick of the heat pipe because of fluid compatibility.

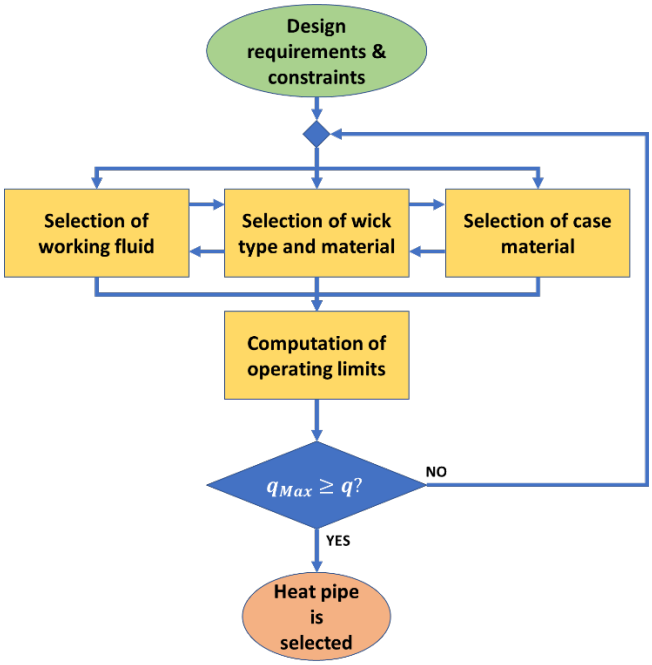

Figure 6: Heat Pipe sizing process

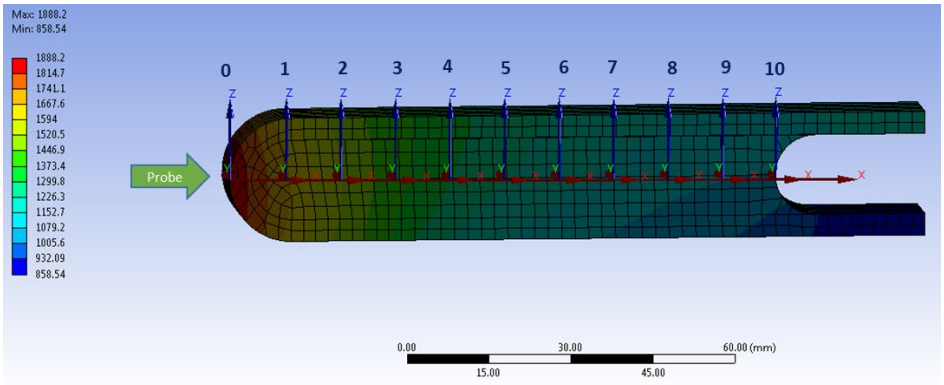

Figure 7: Crotch internal thermal environment

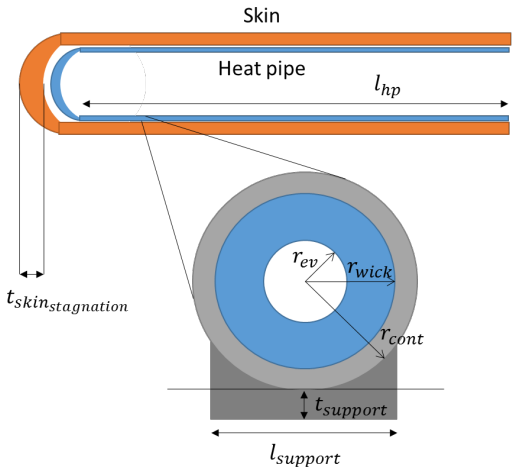

Figure 8: Most promising heat pipe arrangement

The possibility of replacing Nickel (Ni) with other materials such as Aluminium (Al), Steel, Iron (Fe), Copper (Cu) or Tungsten (W) was not assessed since no results were found on compatibility verification. Titanium (Ti) is instead incompatible with Potassium (K).

The selected driving fluid is Potassium (K) which is characterized by a density of 2.08 kg/m^3 in the vapour phase of around 1420 K and a thermal conductivity in (W/mK) of 52 W/mK for liquid Potassium (K) at 340 K and 22 W/mK for vapor Potassium (K) at around 1420 K. The reference value for specific heat at constant pressure for the fluid is 750 J/kgK.

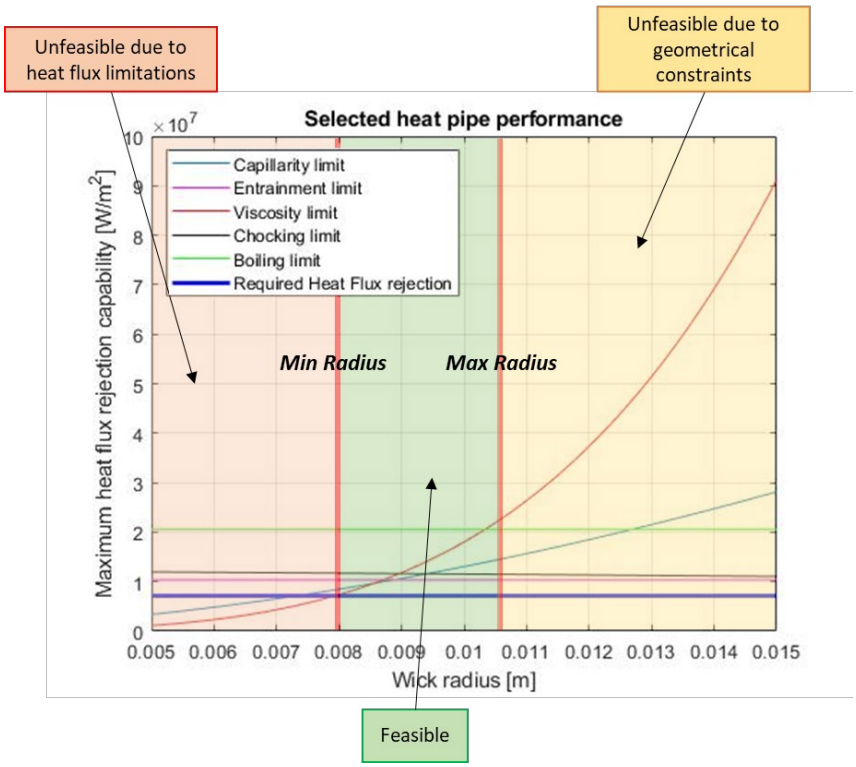

Figure 9. Design space for the selected heat pipe architecture and constraints

Figure 9 summarizes the results achieved so far for the preliminary design of the air-intake heat-pipe. It shows the main design requirements and design space for the selected architecture. In general, the main design requirements are associated to the thermal environment that the heat pipe shall face, in terms of temperature boundaries and heat fluxes, but they can include also geometrical arrangement as well as orientation of the pipe. Once the problem is characterized, it is possible to identify suitable working fluid and materials for both wick and container. Identification of fluid and materials have mutual influence because of compatibility reasons and operational limitations depending on heat pipe architecture. It is thus possible to define several criteria that shall be satisfied to guarantee the feasibility of the solution, as listed hereafter:

1. $T_{fluid_{melting}} < T_{condenser}$;
2. $T_{fluid_{boiling}} < T_{evaporator}$;
3. $T_{fluid_{critical}} > T_{evaporator}$;
4. $p_{fluid_{critical}} > p_{evaporator}$;
5. Container and wick materials shall be compatible with the fluid;
6. Container and wick materials shall be compatible with the thermal environment;
7. Heat pipe architecture shall be compatible with geometrical arrangement.

As soon as the architecture satisfies the aforementioned criteria, it is possible to compute heat flux limitations associated to the selected arrangement. Particularly, in order to evaluate the maximum heat flux managed by a specific heat pipe, the model focuses on the computation of:

- $q_{Max_{capillarity}}$, the maximum heat flux that can be rejected by the heat pipe considering properties of the fluid, geometrical arrangement and dimension of the heat pipe (in W/m^2);
- $q_{Max_{entrainment}}$, the maximum heat flux that can be rejected by the heat pipe considering entrainment phenomena. This basically happens when shear forces applied by vapor on liquid

are above the surface tension of the liquid, which is captured by vapor flows and sent back to the condenser, without reaching the evaporator (in W/m^2);

- $q_{Max_{viscosity}}$, the maximum heat flux that can be rejected by the heat pipe when the pressure drop in the evaporator is so high to prevent the vapor to flow in the condenser (in W/m^2);
- $q_{Max_{chocking}}$, the maximum heat flux that can be rejected by the heat pipe when vapor reach sonic condition (in W/m^2);
- $q_{Max_{boiling}}$, the maximum heat flux that can be rejected by the heat pipe avoiding evaporator dry out due to fluid nucleation fluid boiling in the wick (in W/m^2).

The necessary condition for a heat pipe architecture to be validated is the satisfaction of additional criteria concerning maximum heat fluxes, as listed hereafter:

$$q_{Max_{capillarity}} > q_{Max}$$
$$q_{Max_{entrainment}} > q_{Max}$$
$$q_{Max_{viscosity}} > q_{Max}$$
$$q_{Max_{chocking}} > q_{Max}$$
$$q_{Max_{boiling}} > q_{Max}$$

The main output of the process is thus a design space relating heat pipe performance, dimensions and geometrical constraints as reported in Figure 9.

4.2 Tungsten leading edge- High Emissivity Paint

A first thermal analysis has been performed by considering a tungsten crotch leading edge cooled by heat pipes and coated by high emissivity paint, using the arrangement reported in Fig. 10. Considering the results of the simplified and stationary evaluation of the heat-pipe effectiveness, a representative subtractive heat flux with a peak of about 1 MW/m2, has been modelled and used as input (see Fig. 11a). Figure 11 b shows the temperature map at maximum time instant reaching a peak of 1319°C which is expected to happen at 3242s that is widely below the maximum operative temperature (1800°C). Fig. 11c shows respectively the thermal map at maximum time instant and the comparison of the thermal evolution on the leeside and windside CMC panels. Please, notice that the resulting surface temperatures are always widely below the maximum operative temperature of 1600°C, thus the reference design would be safe.

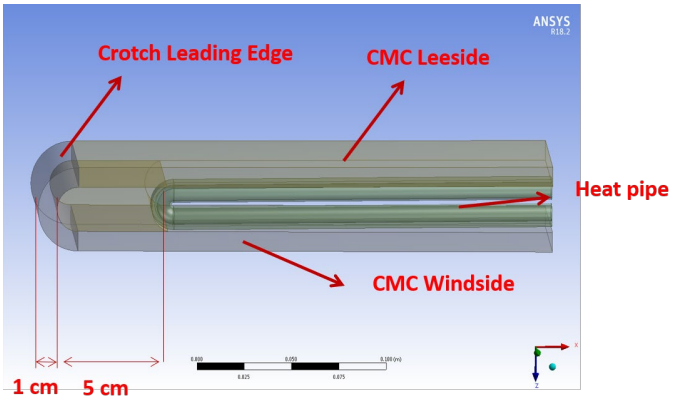

Figure 10. Crotch geometry basic layout

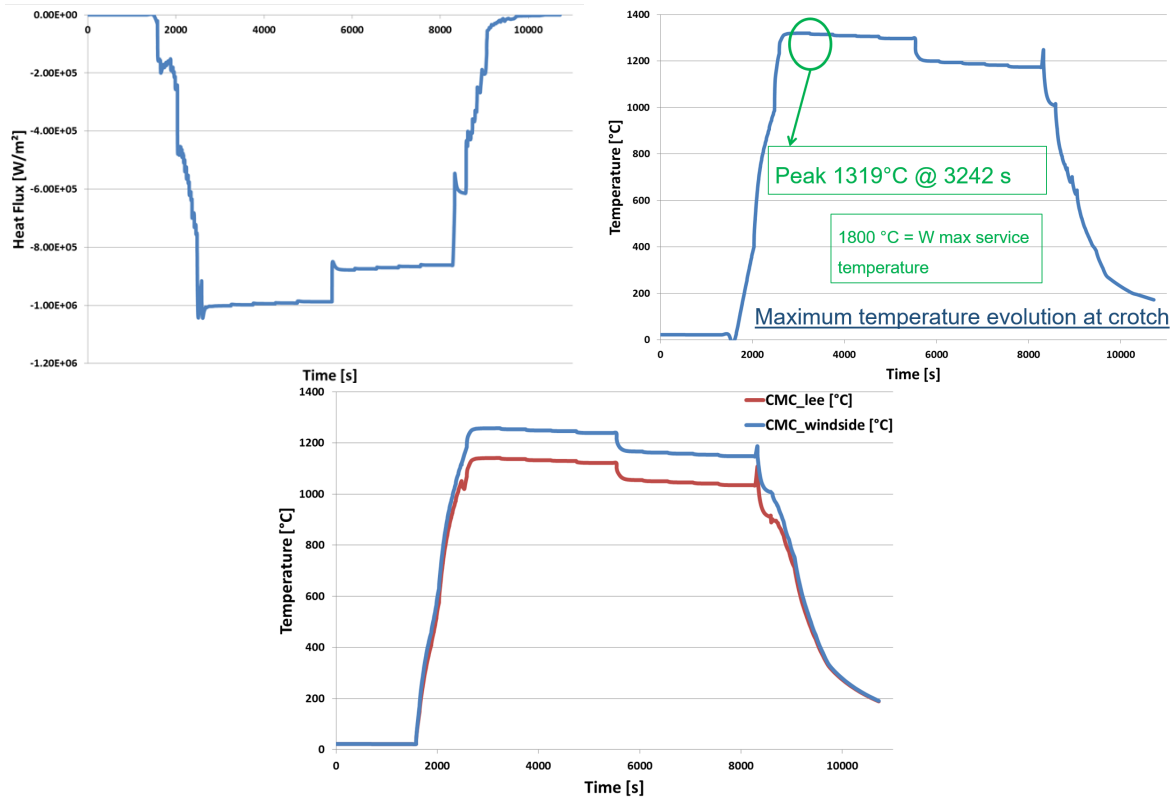

Figure 11. (a) Subtractive Heat Flux evolution (b) Maximum temperature evolution at crotch; (c) Maximum temperature evolution on CMC panels

4.3 Tungsten leading edge- Low Emissivity Paint

A second thermal analysis has been performed by considering the same heat pipe arrangement, but with a tungsten leading edge coated by low emissivity paint (about 0.6). Considering that the heat-pipe arrangement is not changing, the same subtractive heat flux has been considered. Figure shows the temperature map at maximum time instant reaching a peak of 1379°C at 3094s that is widely below the maximum operative temperature (1800°C). Figure 12a shows the maximum temperature evolution at crotch w.r.t emissivity. Both cases are safe Figure 12b and Figure 12c show respectively the thermal map at maximum time instant and the thermal evolution on the leeside and windside CMC panels w.r.t emissivity. Temperature are always widely below the maximum operative temperature of 1600°C, so this design would be safe.

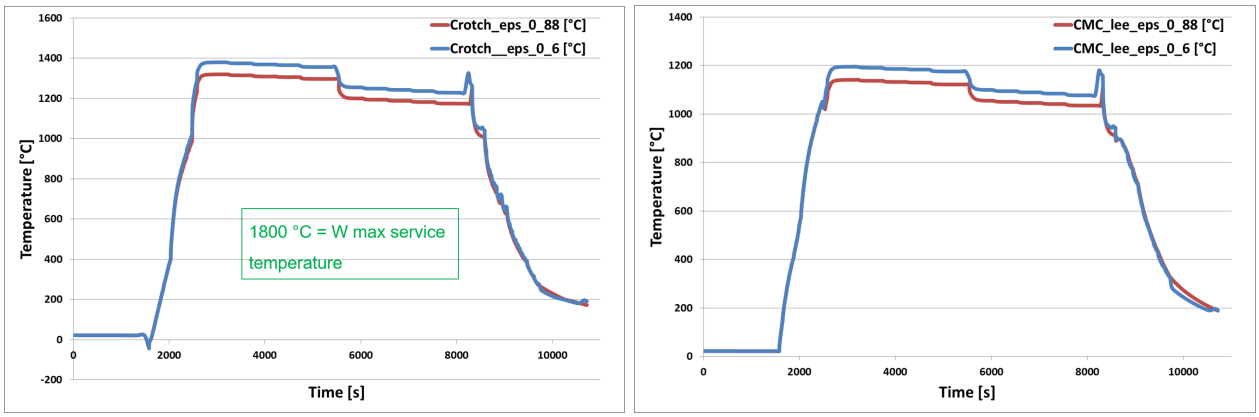

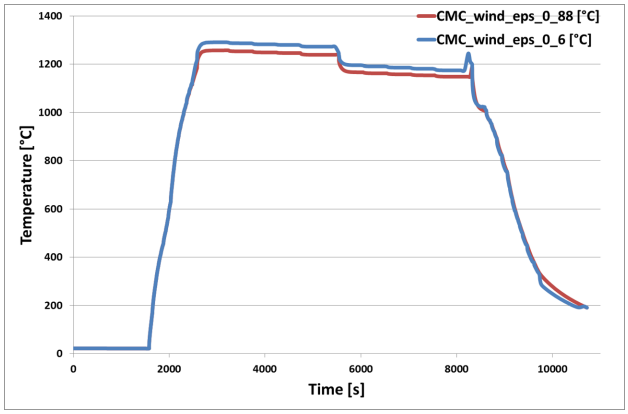

Figure 12. (a) Maximum temperature evolution at crotch w.r.t emissivity; (b) Maximum temperature evolution at CMC leeside panel w.r.t emissivity; (c) Maximum temperature evolution at CMC windside panel w.r.t emissivity

4.4 CMC leading edge

A third set of thermal analyses has been performed by considering a full CMC leading edge cooled by heat pipes (same arrangement as before). Firstly, four different simulations have been performed varying the subtractive heat fluxes from the pipe. This allows checking the effect on maximum temperature on the crotch. Figure 13a shows the different fluxes whose peaks range from 700 kW/m2 for run 1 to about 950 kW/m2 for run 4. Figure 13b shows the corresponding results in terms of maximum temperature on the crotch. It is clear that CMC acts as a very effective thermal barrier. Indeed, an increment in subtractive heat fluxes of the 25%, results in a 4.85% temperature reduction. Finally, run4 conditions are retained because it represents the one that keeps the CMC temperature under the theorical service operative temperature fixed at 1600°C. Figure 12a shows the thermal map on CMC leading edge at maximum time instant. The temperature reaches, in this case, a peak value of 1598°C at 2634s. Fig. 12b show the thermal behaviour of the CMC panels.

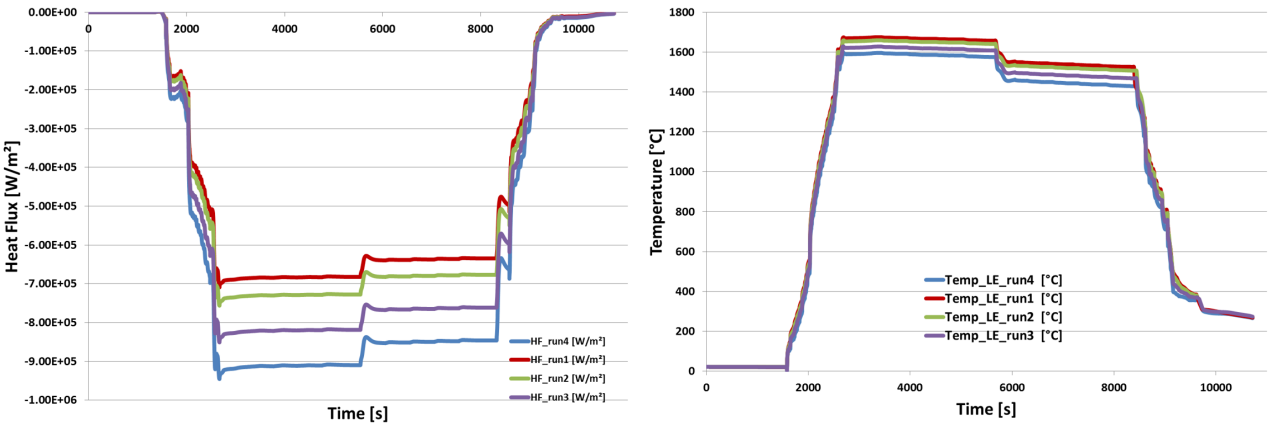

Figure 13. (a) Subtractive heat fluxes from heat pipe; (b)Maximum temperature evolution at CMC crotch w.r.t different subtractive heat fluxes

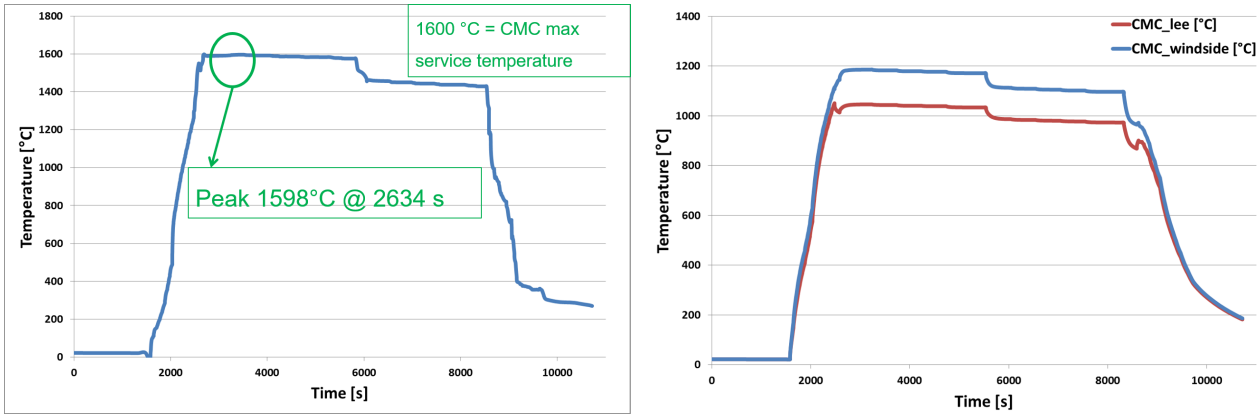

Figure 14. (a) Maximum temperature evolution at CMC crotch (b) Maximum temperature evolution at CMC leeside and windside panel

In conclusion, analysing the three main Thermal Protection Systems Layout, the optimum crotch design shall consist in a main structure made of CMC with standard high emissivity (ε=0.8). The heat pipe arrangement shall be able to provide a subtractive heat flux with a peak of about 0.9 MW/m^2.

5. Thermal Design verification: Heat Pipe effectiveness

In order to verify the hypotheses reported in the previous Section and related to the subtractive heat flux provided by the selected heat pipe arrangement, a numerical model has been set up.
The heat pipe operations can be described by a lumped parametric model based on the electrical analogy. Solid components and fluidic domains are subdivided into a number of finite sub-volumes. The thermal properties and the average temperature of each sub-volume are assumed to be concentrated in the relative node. Nodes are connected to each other by means of resistive, capacitive and inductive elements modelling different physical phenomena.
Thus, the physical system is reduced to an electrical network where the current and the tension represent respectively the thermal flux and the temperature difference between two nodes. Appling Ohm's law and Kirchhoff's law it is possible to obtain an ordinary differential equation governing each node, so the overall transient problem can be reduced to a linear system of ODE easily implemented in a code and numerically solved.

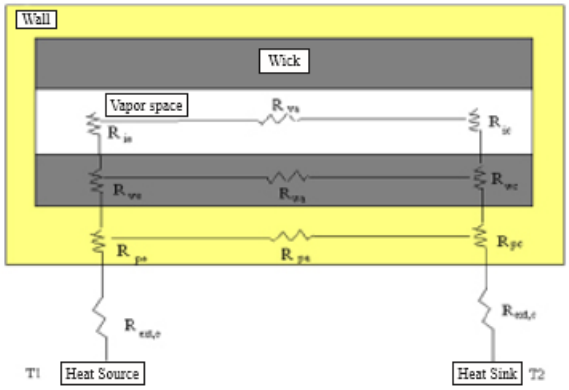

Figure 15. Heat pipe lumped parametric model

Following the simplifications, the total power transported by the heat pipe can be defined:

$$Q = \frac{K_{eff} * A * \Delta T}{L_{eff}} \quad (4)$$

Where

K_{eff}= Effective thermal conductivity [W/m.K],
L_{eff} = Effective length = ($L_{evaorator}$ + $L_{condenser}$)/2 + $L_{adiabatic}$ [m]
A = Cross-sectional area [m_2]
ΔT = Temperature difference between evaporator and condenser sections [°C]

When the Potassium in evaporator zone reaches its boiling temperature, the heat pipe is activated. The heat transport is driven predominantly by convection in pipe fluids which is the main heat transfer mechanism. However, considering that heat pipes are two-phase heat transfer devices, they do not have relatively constant thermal conductivities like solid materials, an effective thermal conductivity is used. The equation used to calculate the effective thermal conductivity for a heat pipe is:

$$\boldsymbol{K_{eff} = \frac{Q_{in} * L_{eff}}{A * (T_{evap} - T_{cond})}} \quad \textbf{(5)}$$

Where:

Q_{in} is the heat flux input,
A is the cross-sectional area of the heat pipe
$L_{eff}=L_{adia}+0,5(L_{evap}+L_{cond})$ is an effective transport length

5.1 Verification of the selected TPS air-intake configuration

The numerical model set up to verify the effectiveness has been applied to all the case-studies previously described. Hereafter, the results achieved for the most promising configuration, i.e. the one exploiting CMC at high-emissivity painting of the selected configuration has been performed by considering a full-CMC leading edge cooled with heat pipe. Figure 16a shows the results in terms of maximum temperature on the CMC leading edge for without heat-pipe activation (blue line) and with pipe heat transfer cooling effect, computed by the numerical model (yellow line). The temperature reaches values of 1830°C when the analysis is carried out without considering the pipe heat transfer cooling effect, instead 1662°C is reached when pipe activation is considered. Complementary, Figure 16b shows the corresponding results in terms of maximum temperature at the interface between the crotch and the pipe structure. The temperature reaches a value of 1732°C when the analysis is carried out without considering Pipe heat transfer cooling effect, instead 1421°C is reached when pipe activation is considered.
Most importantly, Figure 17 shows the effective subtractive heat flux derived by Pipe activation evaluated through the parametric model. The average effective subtractive heat flux is about 0.72 MW/m^2 and it includes both the conductive and convective heat flux subtracted by pipe. The average heat flux of the analysis, considering only active conduction heat transport, derives only by conduction mechanism, so the difference between the effective subtractive heat flux derived by Pipe activation and the heat derived only by conduction mechanism represents the convective subtractive heat flux derived by Pipe activation. The amount of the convective heat flux subtracted is about 0.4 MW/m^2.
Please, it is important to notice that the value of the effective subtractive heat flux derived by Pipe activation (0.72 MW/m^2) is well in line with the most conservative value (0.7 MW/m^2) hypothesized during the thermal design approach.

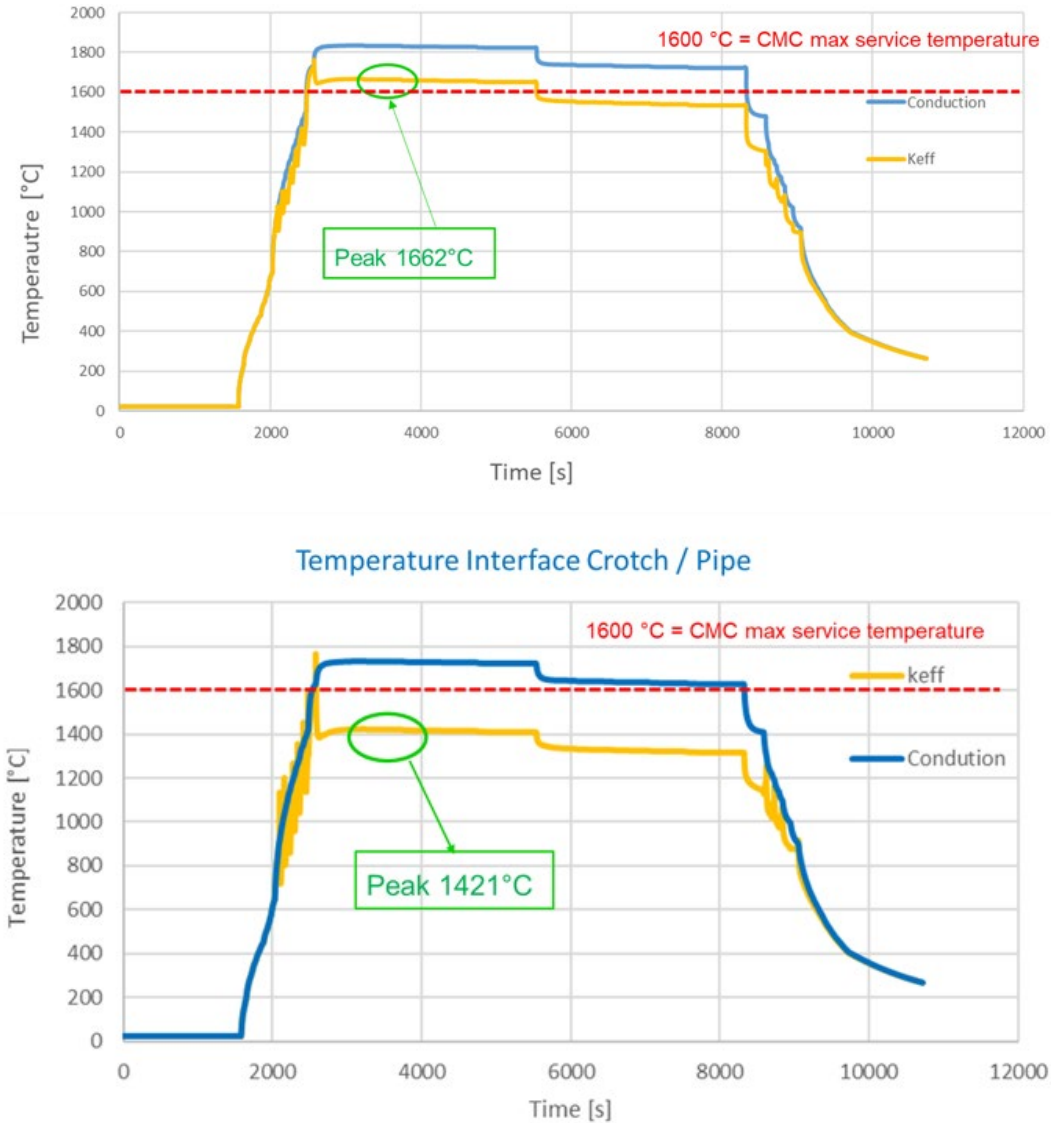

Figure 16. (a) Maximum temperature evolution at CMC Leading edge w.r.t different thermal analysis; (b) Maximum temperature evolution at Interface Crotch/Pipe w.r.t different thermal analysis

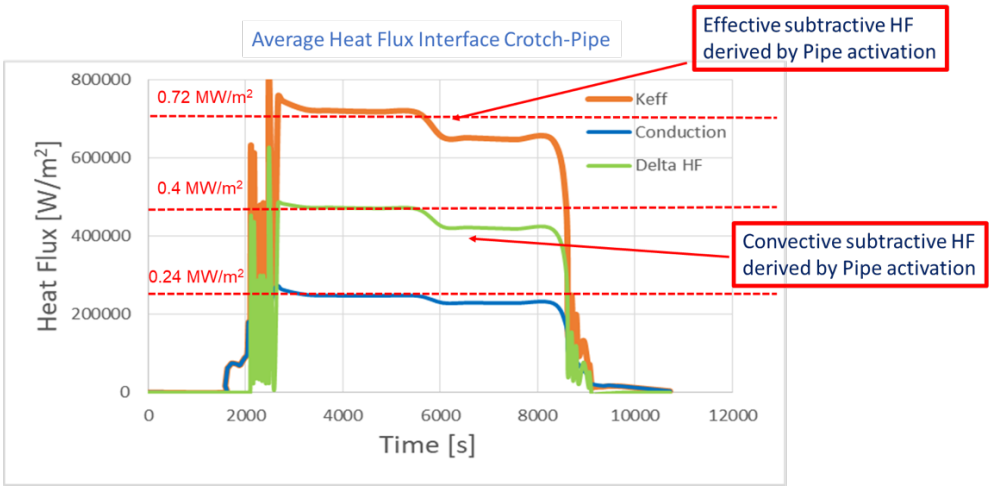

Figure 17. Average Heat Flux evolution at crotch-Pipe interface w.r.t different thermal analysis

6. Conclusions and future work

This paper has presented the methodology and the preliminary results achieved in the framework of the H2020 STRATOFLY Project on the design of the Thermal Protection System of the MR3 vehicle, with specific focus on the air-intake area, where the highest temperatures are foreseen. The results of the aero-thermal assessment performed throughout the trajectory with engineering formulations as well as with dedicated CFD analysis clearly indicate the air-intake leading edges as the most critical area, thus dedicated Thermal Protection System alternatives have been explored. Specifically, solutions coupling high-temperature materials (mainly CMC and tungsten with different emissivity paints) with Liquid Metals Heat Pipe arrangements have been modelled.
Eventually, the effectiveness of the designed solutions is verified with detailed numerical simulations, where the electrical analogy is used to define a parametric model able to estimate the effective subtractive heat flux provided by the designed heat-pipe arrangement. The design which includes the air-intake main structure made of CMC material and integrating Nickel - Potassium heat pipe results to be the most promising solution to withstand the high thermal loads experienced by STRATOFLY MR3 throughout its Mach 8 long-haul route.
The results disclosed in this paper are highly interesting both rom the theoretical and from the practical standpoints. Indeed, from the theoretical standpoint, this paper suggests an innovative methodology for the selection of a reliable Thermal Protection System applicable since the earliest design stages. In addition, the parametric model for heat pipe design verification, based on the electrical analogy is highly interesting. Complementary, from the practical standpoint, the possibility to exploit liquid metals heat pipes for hypersonic transportation system (an idea that moves back to the NASP project) shall be further investigated, to better understand the limits of operations as well as the thermal behaviour of the air-intake during the transient start-up phases.

7. Contact Author Email Address

mailto: r.scigliano@cira.it

8. Copyright Statement

References

[1] Steelant J., Varvill R., Defoort S., Hannemann K., Marini M., “Achievements Obtained for Sustained Hypersonic Flight within the LAPCAT-II Project”, AIAA-2015-3677, 20th AIAA International Space Planes and Hypersonic Systems and Technologies Conference, Glasgow, Scotland, 6-9 July 2015.

[2] J. Steelant. ATLLAS: Aero-thermal loaded material investigations for high-speed vehicles. In: 15th AIAA International Space Planes and Hypersonic Systems and Technologies Conference. 2008. p. 2582.

[3] J. Steelant. et al., Conceptual Design of the High-Speed Propelled Experimental Flight Test Vehicle HEXAFLY, *20th AIAA International Space Planes and Hypersonic Systems and Technologies Conference*, Glasgow, Scotland, AIAA 2015-3539

[4] S. Di Benedetto et al., Multidisciplinary Design and Flight Test of the HEXAFLY-INT Experimental Flight Vehicle Hexafly-Int, *HiSST: International Conference on High-Speed Vehicle Science Technology*, Moscow, Russia, 2018

[5] JY Andro, R. Scigliano, A. Kallembach, J. Steelant, Thermal Management of the Hexafly-Int Hypersonic Glider, *HiSST: International Conference on High-Speed Vehicle Science Technology*, Moscow, Russia, November 2018

[6] R. Scigliano, S. Di Benedetto, M. Marini, V. Villace, J. Steelant, Hexafly-Int Hypersonic Vehicle Thermal Protection System Design, *71st International Astronautical Congress (IAC) – The CyberSpace Edition*, 12-14 October 2020, IAC-20-56572.

[7] Roberto Scigliano , Giuseppe Pezzella, Sara Di Benedetto, Marco Marini, Johan Steelant, “HEXAFLY-INT Experimental Flight Test Vehicle (EFTV) Aero-Thermal Design”, *ASME International Mechanical*

Engineering Congress & Exposition (IMECE), IMECE2017-70392, Tampa, FL, USA, November 3-9, 2017.

[8] Viola, N., Fusaro, R., Saracoglu, B., Schram, C., Grewe, V., Martinez, J., ... & Fureby, C. (2021). Main challenges and goals of the H2020 STRATOFLY project. Aerotecnica Missili & Spazio, 1-16.

[9] Viola, N., Fusaro, R., Gori, O., Marini, M., Roncioni, P., Saccone, G., Saracoglu, B., Ispir, A.C., Fureby, C., Nilsson, T., Ibron, C., Zettervall, N., Bates, K.N., Vincent, A., Martinez-Schram, J., Grewe, V., Pletzer, J., Hauglustaine, D., Linke, F., Bodmer, D. Stratofly MR3 – how to reduce the environmental impact of high-speed transportation, (2021) AIAA Scitech 2021 Forum, pp. 1-21.

[10] Langener, T., Erb, S., Steelant, J., & Flight, H. (2014). Trajectory Simulation and Optimization of the LAPCAT MR2 Hypersonic Cruiser Concept. *ICAS 2014*, *428*.

[11] Viola,N.; Roncioni,P.; Gori, O.; Fusaro, R. Aerodynamic Characterization of Hypersonic Transportation Systems and Its Impact on Mission Analysis. Energies 2021,14,3580. https://doi.org/10.3390/en14123580

[12] Zoby, E. V., Moss, J. N., & Sutton, K. (1981). Approximate convective-heating equations for hypersonic flows. *Journal of Spacecraft and Rockets*, *18*(1), 64-70.

[13] R. Scigliano, V. De Simone, M. Marini, P. Roncioni, R. Fusaro, N. Viola, Preliminary Finite Element Thermal Analysis of STRATOFLY Hypersonic Vehicle, 23rd AIAA International Space Planes and Hypersonic Systems and Technologies Conference - AIAA HYPERSONICS 2020, March 10-12, 2020, Montreal, Quebec, Canada.

[14] R. Scigliano, M. Marini, P. Roncioni, R. Fusaro, N. Viola, STRATOFLY High-Speed Propelled Vehicle Preliminary Aero-Thermal Design, *International Conference on Flight Vehicles, Aerothermodynamics and Re-Entry Missions and Engineering FAR 2019, Monopoli (Italy)*, 30th September - 3rd October 2019.

[15] R. Scigliano, M. Marini, R. Fusaro, N. Viola, Preliminary Aero-Thermal Assessment of the High-Speed Propelled Vehicle STRATOFLY, *32nd ISTS (International Symposium on Space Technology and Science) & 9th NSAT (Nano-Satellite Symposium),* Fukui (Japan), June 2019.

[16] B. Zahuri, Heat Pipe Design and Technology – A practical approach, CRC Press, New York, 2011

[17] P. J. Brennan, E. J. Kroliczek, Heat Pipe Design Handbook – Volume I, B&K Engineerin Inc., Towson (MD), 1979.

[18] A. Faghri, Heat Pipe Science and Technology, CRC Press, New York, 1995.